

## In vivo Doppler optical coherence tomography of mucocutaneous telangiectases in hereditary hemorrhagic telangiectasia

Shou-jiang Tang, MD, Maggie L. Gordon, BSc, Victor X. D. Yang, PhD, Marie E. Faughnan, MD, MSc, Maria Cirocco, BScN, Bing Qi, PhD, Emily Seng Yue, Geoffrey Gardiner, MD, Gregory B. Haber, MD, Gabor Kandel, MD, Paul Kortan, MD, Alex Vitkin, PhD, Brian C. Wilson, PhD, Norman E. Marcon, MD

**Background:** Hereditary hemorrhagic telangiectasia is characterized by mucocutaneous telangiectases and visceral arteriovenous malformations. Knowledge is limited concerning the development hemodynamics of mucocutaneous telangiectases. Doppler optical coherence tomography can demonstrate microvascular blood flow at flow rates as low as 20  $\mu\text{m}/\text{second}$ , which is up to approximately 100 times more sensitive than Doppler US. The aims of this study were to collect in vivo Doppler optical coherence tomography images of mucocutaneous telangiectases and normal surrounding mucosa and skin, and to gain experience for an in vivo GI endoscopic study. It was hypothesized that visibly normal areas may have occult telangiectases and that mucocutaneous telangiectases that have bled may have a higher rate of blood flow than mucocutaneous telangiectases with no history of bleeding.

**Methods:** Twelve patients with hereditary hemorrhagic telangiectasia and mucocutaneous telangiectases were studied. Two to 3 visible mucocutaneous telangiectases on the digits, lips, and tongue were imaged with Doppler

optical coherence tomography, along with visually normal surrounding areas at each site. The Doppler optical coherence tomography images were obtained in 0.5 second by using 1310 nm light.

**Results:** A total of 67 mucocutaneous telangiectases from the 12 patients were imaged (38 digit, 16 lip, 13 tongue). Blood flow was demonstrated within every mucocutaneous telangiectasis imaged. Doppler optical coherence tomography did not identify any abnormal vasculature within visually normal areas. Mucocutaneous telangiectases with a history of bleeding ( $n = 18$ ) were situated closer to the surface, compared with mucocutaneous telangiectases with no bleeding history ( $n = 49$ ), but there was no difference in the Doppler flow appearance.

**Conclusions:** Visually normal areas in patients with hereditary hemorrhagic telangiectasia did not appear to have abnormal vasculature. Mucocutaneous telangiectases with a history of bleeding were more superficial but were otherwise similar to mucocutaneous telangiectases with no bleeding history.

Hereditary hemorrhagic telangiectasia (HHT), or Osler-Weber-Rendu disease, is an autosomal dominant disorder with an estimated prevalence of 1:8000.<sup>1,2</sup> Hereditary hemorrhagic telangiectasia is characterized by abnormal vasculature that manifests as mucocutaneous telangiectases (MCT) and visceral arteriovenous malformations (AVM).<sup>1,2</sup> Classically, MCTs are described as purple stains, ranging from pinpoint to pea size. In one study, MCTs were present in 74% of patients with HHT, and 30% to 40% had MCTs on their hands, lips, and tongue.<sup>3</sup> Visceral vascular beds often have AVMs, including the lungs, cerebrum, and liver. Recurrent epistaxis and GI hemorrhage are common in patients with HHT.<sup>4,5</sup> GI bleeding has been reported in 15% to 30% of patients as they age.<sup>3,4</sup> Current treatment for bleeding MCTs involves some form of local thermal therapy.<sup>3-6</sup> Unfortunately, recurrence of mucocutaneous bleeding is common despite treatment.

Optical coherence tomography (OCT) is a novel imaging technique that is analogous to US imaging, although near-infrared light is used instead of sound. Optical coherence tomography can provide in vivo, real-time images with extremely high spatial resolu-

Received March 19, 2003. For revision May 23, 2003. Accepted June 13, 2003.

Current affiliations: Center for Therapeutic Endoscopy and Endoscopic Oncology, Division of Respiratory Medicine, Department of Medicine, Department of Pathology, St. Michael's Hospital, Department of Medical Biophysics, Department of Radiation Oncology, University of Toronto, Division of Medical Physics, Ontario Cancer Institute, Princess Margaret Hospital, Photonics Research, Ontario.

Reprint requests: Norman E. Marcon, MD, Center for Therapeutic Endoscopy and Endoscopic Oncology, Victoria Wing 16-062, St. Michael's Hospital, Toronto, Ontario, Canada M5B 1W8.

Copyright © 2003 by the American Society for Gastrointestinal Endoscopy

0016-5107/2003/\$30.00 + 0

PII S0016-5107(03)01978-3

Table 1. Patient characteristics

Patient	Gender	Age	Family history	Age at onset	MCTs on examination			MCT history of bleeding					HHT involment		Comorbid conditions
					Digits	Lip	Tongue	Nose	GI	Digits	Lip	Tongue	PAVM	Stroke	
1	M	38	+	<10	2-3	5-10	2	+	−	−	−	−	+	+	HTN, asthma
2	M	40	+	30-40	1-2	5-10	2	+	−	−	+	+	−	−	
3	M	43	+*	30-40	10-15	10	10	+	−	−	+	−	+	−	
4	M	53	+	10-20	30-50	5-10	>20	+	+	−	+	+	+	−	Celiac disease
5	M	53	+	40-50	5-10	0	2	+	−	+	−	−	−	−	
6	F	54	+	40-50	25-50	10	0	+	−	+	−	−	+	+	
7	F	55	+*	20-30	25-50	>10	>10	+	−	−	+	−	+	−	HTN
8	F	58		<10	25-50	50	25	+	+	−	+	−	+	+	
9	M	62	+	20-30	10-15	1	5-10	+	−	+	+	+	−	−	
10	M	64	+*	<10	>50	>10	>10	+	−	−	+	+	+	−	Colon cancer
11	M	67	+	<10	>50	<10	5	+	−	−	−	−	+	−	
12	F	67	+	<10	5-10	2	2	+	+	−	−	+	−	−	

MCT, Mucocutaneous telangiectases; HHT, hereditary hemorrhagic telangiectasia; PAVM, pulmonary arteriovenous malformation; HTN, hypertension.  
\*Positive for type 1 HHT gene.

Table 2. Characteristics of the MCTs imaged in HHT patients

		No history of bleeding				History of bleeding				p Value
	Size	Pinpoint	Small	Large	All lesions	Pinpoint	Small	Large	All lesions	
Digits	Number	15	20	0	35	3	0	0	3	<0.05
	Depth (µm)	100	73		84 (24)	29			29 (51)	
Lips	Number	3	4	0	7	0	7	2	9	0.13
	Depth (µm)	132	125		128 (44)		105	88	101 (21)	
Tongue	Number	0	6	1	7	0	4	2	6	0.20
	Depth (µm)		186	30	172 (85)		117	132	122 (29)	

Doppler signals, indicating high blood flow volume and/or velocity, were observed in 100% of the imaged MCTs; MCTs were classified as pinpoint (diameter <0.3 mm), small (0.3-2.0 mm), or large (>2 mm). The lesional depth is expressed as mean (SD).  
MCT, Mucocutaneous telangiectases; HHT, hereditary hemorrhagic telangiectasia.

tion ( $\approx$ 5-10 µm) and imaging depths of approximately 2 mm.<sup>7</sup> Optical coherence tomography uses the coherence properties of near-infrared, broadband light sources to examine intact biologic tissues in vivo and in vitro without injury or damage to the tissues.<sup>8-13</sup> Similar to Doppler US, Doppler optical coherence tomography (DOCT) uses OCT information to detect subsurface motion, such as microvascular blood flow, in living specimens.<sup>12</sup> The spatial resolution and the velocity sensitivity of OCT are about 10 times better than high-frequency US, making OCT an ideal modality for studying subsurface microcirculation within approximately the upper 2 mm of tissue.

Animal and human experiments have been conducted to evaluate the ability of DOCT to detect microvasculature and to monitor therapeutic responses. For example, DOCT has been used to monitor rat and murine tumors treated with laser thermal therapy and photodynamic therapy,<sup>14,15</sup> and port wine stains treated by photocoagulation.<sup>12</sup> These results suggest that DOCT can reliably detect microcirculation and monitor changes in blood flow during treatment.

Knowledge about MCT in HHT is limited. For example, it is unknown whether visibly normal areas have tiny telangiectases or what distinguishes lesions that tend to bleed from lesions that do not. To address these questions, DOCT was used to investigate the structure and hemodynamics of MCTs in HHT, as well as visually normal skin or mucosa in patients with HHT. Knowledge and experience in studying these readily available MCTs would help to translate DOCT into endoluminal applications. This information could guide the development of hemostatic therapy, and DOCT may be useful for guiding and monitoring such treatment.<sup>9,12,13</sup> Furthermore, DOCT may provide knowledge about subsurface hemodynamics in neovasculature associated with luminal dysplasia and other microvascular lesions such as portal hypertensive gastroenteropathy and gastric antral vascular ectasia (GAVE or “watermelon” stomach).

PATIENTS AND METHODS

Twelve patients (8 men, 4 women, mean age 55 [10.0] years) with a definite clinical diagnosis of HHT with

MCTs were recruited from consecutive patients seen at the HHT clinic at St. Michael's Hospital, Toronto, Canada. Four normal control subjects also were included in the study. Our institutional ethics review board approved the study, and informed consent was obtained from all patients and normal control subjects. A brief clinical history for each patient was recorded before DOCT imaging and included the identification of MCT with and without a history of bleeding (Table 1).

In every patient, two to three telangiectases on the fingers, tongue, and lips were marked nearby with a pen and then imaged by DOCT. In normal subjects, randomly selected spots on the digits, lips, and tongue also were imaged with DOCT. The physician analyzing the DOCT images was blinded to the type of lesion imaged. The MCTs were classified as pinpoint (diameter <0.3 mm), small (0.3–2 mm), or large (>2 mm). Visually normal surrounding areas at each site also were imaged as control sites. In these sites, several DOCT images were obtained at different locations if neither abnormal microstructure nor a Doppler signal was detected. The DOCT imaging of each lesion took approximately one minute. It was performed at room temperature to avoid temperature-related vasodilatation or vasoconstriction. After DOCT imaging, the hands, lips, and tongue were photographed.

#### DOCT system

A DOCT imaging system developed at the Ontario Cancer Institute was used.<sup>15,16</sup> In brief, the system consists of customized fiber-optic probes for the delivery of low-coherence light to the sample and the collection of the light scattered from the skin subsurface structures. The source had a central wavelength of 1310 nm, a spectral width of approximately 60 nm (full-width-half-maximum) and emitted less than 8 mW of power, resulting in no thermal or other damage to the skin and mucosa.<sup>11,17–20</sup> The spatial resolution was 10  $\mu$ m in both the depth and lateral directions, and the typical velocity sensitivity was 20  $\mu$ m/second when imaging 2 mm  $\times$  1.5 mm of tissue at two frames per second.

The DOCT fiber-optic probe was held about 1 to 2 mm over the skin surface (Fig. 1) and tomographical images (field of view, 2 mm lateral  $\times$  1.5 mm deep), with Doppler flow information acquired in approximately 0.5 second.

#### Data analysis

Each patient was assigned a study number to maintain confidentiality and to ensure investigator blinding. Every DOCT image was coded with this study number, imaging date, site-specific information, and lesion size (pinpoint, small, large). Clinicians, DOCT scientists, and a pathologist analyzed the recorded DOCT images independent of the OCT scientist who performed the imaging procedures (M.L.G.). Features on DOCT images that were suggestive of relevant anatomical structures (e.g., normal blood vessels, dilated blood vessels, stratum corneum, and nail root) were identified.

Morphologically distinct structures containing Doppler signals identified by DOCT were considered to be vascular structures.

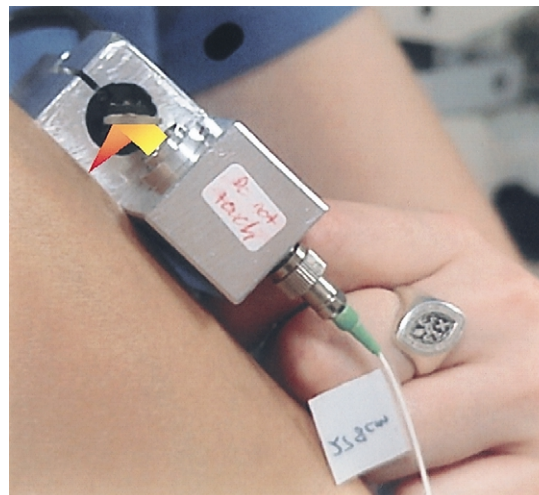


**Figure 1.** Hand-held probe for in vivo DOCT imaging. The unit is 8  $\times$  5  $\times$  2 cm and was held over the skin.

lar structures. The telangiectasia “depth” was defined as the shortest distance between the most superficial edge of a vascular structure and the top layer of the stratum spinosum. The skin surface was not used as a landmark because of the large inter- and inpatient variations in stratum corneum thickness. The lateral dimension of the MCT was defined as the widest spread of the telangiectases on DOCT images. Because of the limited imaging depth (1.5 mm), in the majority of images, the vertical extent of MCT could not be determined, therefore, the height of the MCT was not measured. (Because pathology specimen processing will distort the microvascular shape, pathology was not obtained in this study to correlate with OCT depth measurements).

The MCTs were categorized according to size (as judged by eye, before imaging) and bleeding history (as reported by the patients; Table 2). Blood-flow characteristics in different-sized lesions and in lesions with or without bleeding history were qualitatively compared to determine risk factors for bleeding. The mean and standard deviation are reported for normally distributed data. The two-sided Student *t* test was used to compare the depth measurements in lesions with and without bleeding. For purposes of statistical analysis, the several depth measurements from individual patients were assumed to be independent data points.

## RESULTS

A total of 67 MCTs were imaged in the 12 patients enrolled (Table 1): 38 digit, 16 lip, and 13 tongue. No patient experienced any discomfort or complication during or after DOCT imaging.

#### Structural OCT

The following anatomic structures were clearly and consistently identified in structural OCT images: (1) digits: stratum corneum, stratum lucidum, stratum spinosum, dermal papillae, sweat



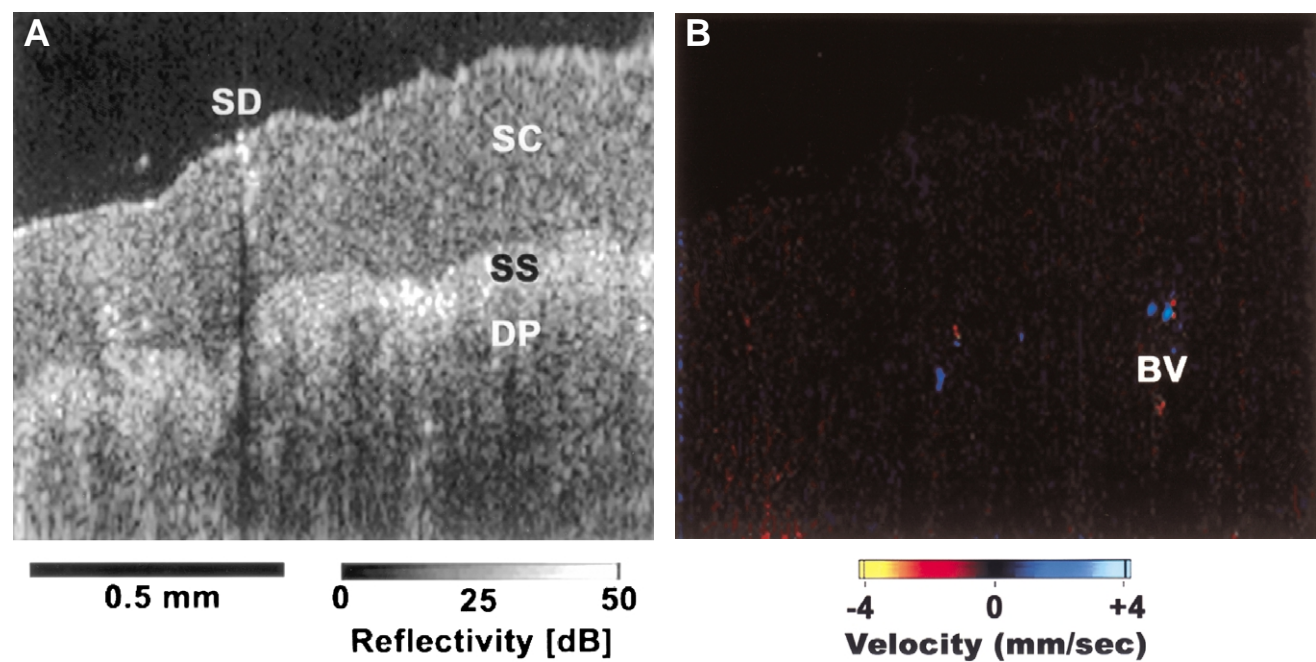


**Figure 2.** **A**, Structural OCT image of normal skin showing thick stratum corneum (SC), stratum spinosum (SS), a sweat duct (SD), and dermal papillae (DP) on palmar surface of finger. **B**, Doppler OCT image of normal human skin showing small blood vessels (BV). Although DOCT usually was not able to detect any blood flow in normal skin, occasionally small vessels were demonstrated.

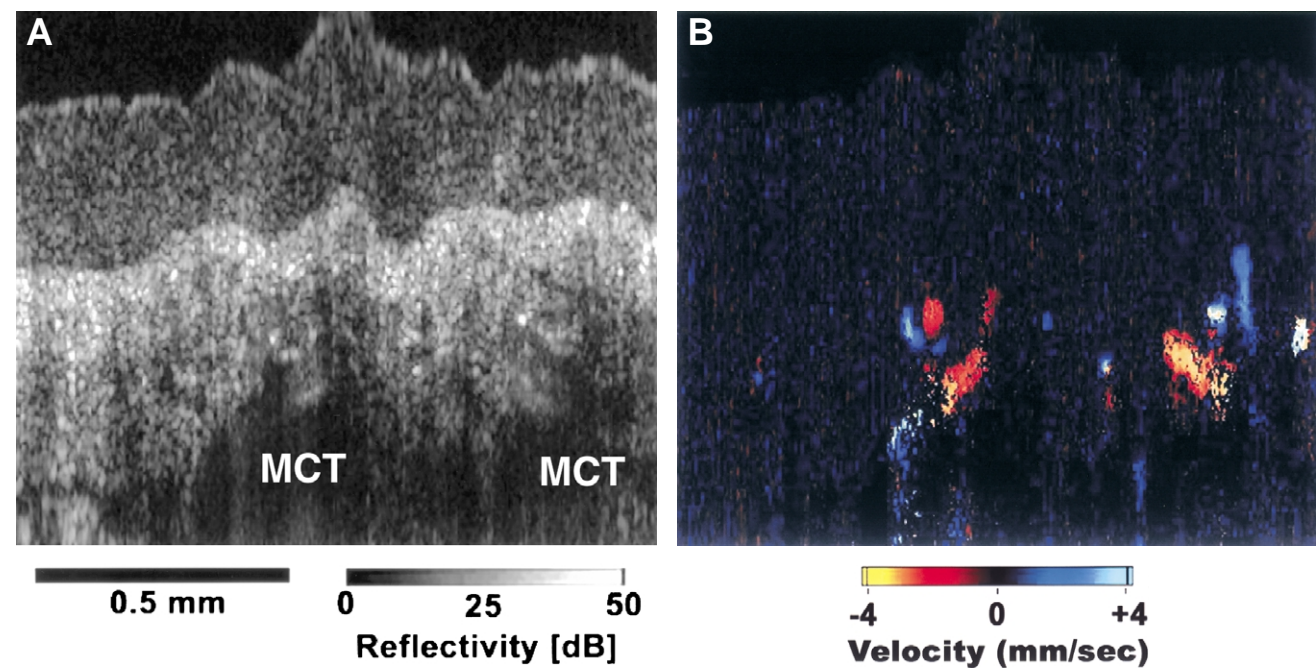


**Figure 3.** **A**, Structural OCT image of MCT lesion (MCT) on palmar surface of digit. **B**, DOCT image of MCT lesion on palmar surface of digit.

glands, and sweat ducts; (2) fingernails: layered nail, dermal papillae in the nail bed, and probable elastic fiber bundles in the nail folds; (3) lips: labial epithelium, lamina propria, labial glands, and normal superficial vessels; and (4) tongue: mucosa, fili-

form and fungiform papillae, and normal superficial vessels. The MCTs appeared as globular shapes in the upper dermis or mucosa in which the normal speckle pattern of stationary tissue was lost because of the flowing blood.

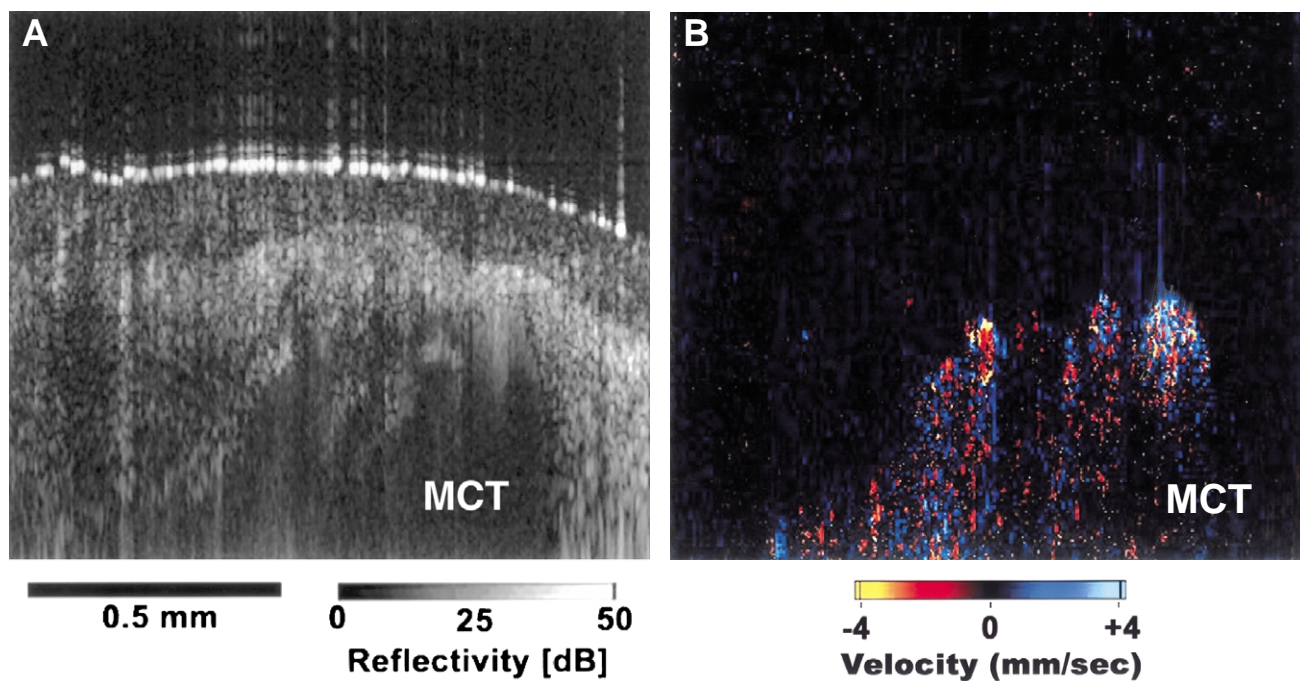


**Figure 4.** A, Structural OCT image of MCT lesion (MCT) on dorsal surface of digit. The speckle pattern seen in stationary surrounding tissue is lost because of blood motion. B, DOCT image in corresponding location showing strong Doppler signals.

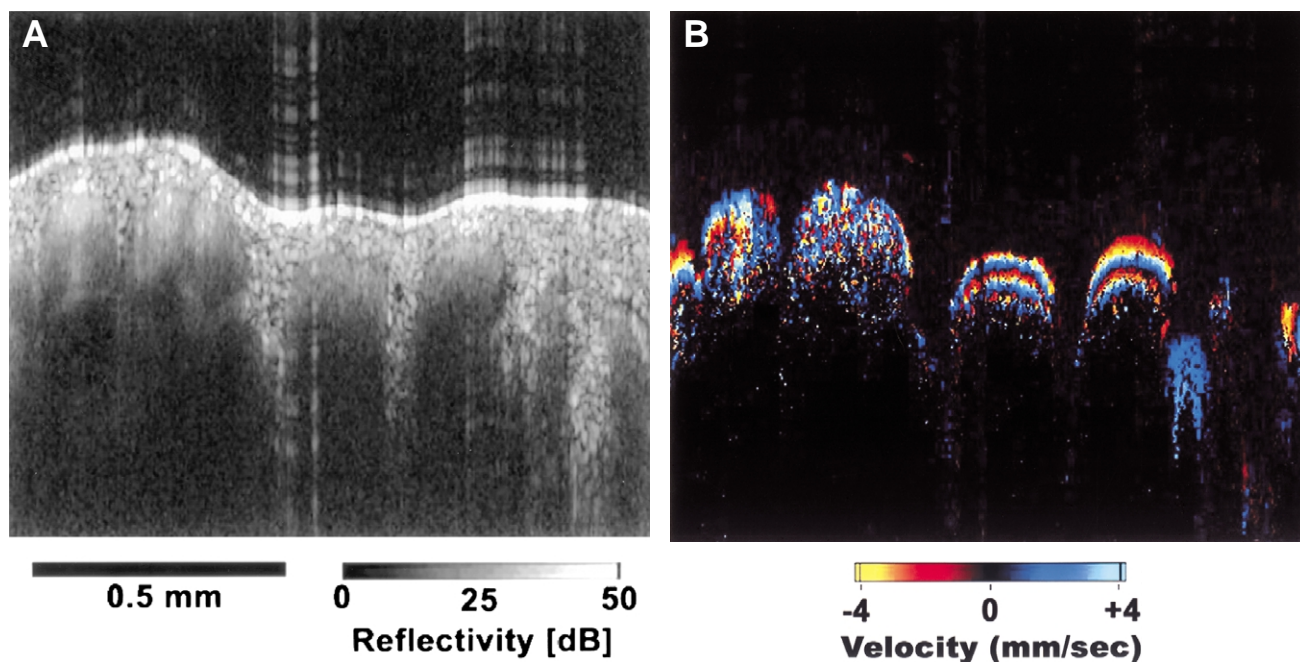


**Figure 5.** A, Structural OCT image of MCT lesion on lip. B, DOCT of MCT lesion on lip. This lesion had a history of bleeding and the lesion depth tended to be shallower than lip lesions with no history of bleeding.

#### Doppler OCT

**Normal blood vessels.** Most normal superficial blood vessels have blood volumes or flow velocities below the sensitivity of our DOCT system. Occasionally, Doppler signals were observed in both normal volunteers ( $n = 4$ ) and in visually normal areas in patients with HHT, especially in the richly vascular lip and tongue.

Doppler OCT of the digits revealed small blood vessels in the upper dermis with diameters 20 to 40  $\mu\text{m}$ , possibly representing arterioles or venules. The lips and tongue had similar small vessels (20-80  $\mu\text{m}$  in diameter). The normal vessels appeared as scattered Doppler spots on the DOCT images without forming well-defined morphologic structures (Fig. 2). Visually nor-



mal areas on the skin of HHT patients did not exhibit any abnormal Doppler signals.

**Mucocutaneous telangiectases.** Although normal superficial blood vessels were seldom detected, blood flow was clearly demonstrated within every scanned MCT (Figs. 3 through 5).

Comparing MCTs that had bled with those that had not, there were no qualitative differences in the Doppler flow appearance. None of the pinpoint-sized MCTs had bled in the past, but size alone did not predict the bleeding history for a lesion. However, proximity to the stratum spinosum was associated with a tendency to bleed, because MCTs with a bleeding history ( $n = 18$ ) were situated closer to the surface than lesions without bleeding history ( $n = 49$ ) (Table 2). Two of the 3 cutaneous telangiectases with a bleeding history penetrated the stratum spinosum layer as seen on DOCT imaging, whereas none of the lesions without a bleeding history extended past the dermis.

Quantitatively, the mean (1 SD) depth of the cutaneous lesions with a bleeding history was 29 (51)  $\mu\text{m}$  ( $n = 3$ ), which was less than for lesions without a bleeding history: 84 (24)  $\mu\text{m}$  ( $n = 35$ ) ( $p = 0.002$ ; two-tailed  $t$  test). For lip lesions, the corresponding values were 101 (21)  $\mu\text{m}$  ( $n = 9$ ) vs. 128 (44)  $\mu\text{m}$  ( $n = 7$ ) ( $p = 0.13$ ); and for tongue lesions, 122 (29)  $\mu\text{m}$  ( $n = 6$ ) vs. 172 (85)  $\mu\text{m}$  ( $n = 6$ ) ( $p = 0.20$ ).

## DISCUSSION

Doppler optical coherence tomography is a new imaging modality that can provide high-resolution, subsurface, nondestructive, microstructural tomographs supplemented with blood flow maps in any area that is accessible to a fiber-optic probe.<sup>12,13</sup> The DOCT may be used to guide and monitor local and endoscopic hemostatic therapies.<sup>9,12,13</sup> The noninvasive microstructural and microvascular imaging capabilities are well suited for MCT examination in patients with HHT. The present study demonstrates that the high blood volume and/or the rapid blood-flow velocity provide discernible Doppler signals from HHT lesions that can be clearly imaged with DOCT. No abnormal Doppler signal or OCT structure was found in normal surrounding mucosa and skin.

The flow velocity threshold of the system is 20  $\mu\text{m}/\text{second}$ . The flow velocity within normal capillaries is approximately 15 to 25  $\mu\text{m}/\text{second}$ , with luminal diameter of 5 to 10  $\mu\text{m}$ ,<sup>21</sup> so that, as observed, our DOCT system could not detect normal capillary blood flow within the dermis. However, superficial arterioles with greater flow velocity or larger diameter may be detected. Optical coherence tomography has demonstrated structural features that are important for clinical staging and management of

superficial diseases,<sup>7-19</sup> and the present study has shown that DOCT can demonstrate abnormal superficial blood vessels.

Mucocutaneous telangiectases were demonstrated unequivocally by DOCT as globular shapes or venous lakes with Doppler signal, representing high-volume and/or high-velocity blood flow. Visibly normal areas in the skin of patients with HHT did not have abnormal structure or Doppler signal. In the skin, there were occasionally a few small vessels 20 to 80  $\mu\text{m}$  in diameter in the upper dermis and significantly more such vessels in the lips and tongue.

Braverman et al.<sup>21</sup> studied 10 cutaneous telangiectatic lesions in HHT by electron microscopy of biopsy tissue after resin processing. Three-dimensional images of these lesions also were constructed. Histologic patterns were found in the HHT lesions that were related to the size of the clinical lesions. Pinpoint lesions had a focal dilation of post-capillary venules with normal smaller venules connected to them. As the lesions enlarged, arterioles became dilated, followed by dramatic venular dilation. These dilated post-capillary venules are believed to eventually bypass the capillary networks and fuse directly with dilated arterioles, forming direct arteriolar-venular communications and large telangiectases.<sup>21</sup> Studies of HHT MCTs involving the tongue and nasal mucosa also have suggested that the dilated subepithelial vessels are post-capillary venules.<sup>22,23</sup> Three-dimensional reconstruction of the hepatic microvasculature of HHT-involved liver revealed that periportal arterioles communicate directly with the ectatic sinusoids, forming arteriovenous shunts that are not present in unaffected livers.<sup>24</sup> Portovenous shunts from dilated portal venous branches are frequent and abnormally large compared with normal liver.

The development of MCTs in HHT has some similarities with normal angiogenesis.<sup>21,25</sup> Angiogenesis has been separated into two phases. The initial phase involves endothelial cell migration, replication and vessel formation; the second phase encompasses small vessel enlargement by expansion.<sup>25,26</sup> The development of HHT MCTs closely resembles the second angiogenesis phase, and it has been suggested that HHT is a reasonable model of the vessel enlargement seen in the second phase of angiogenesis.<sup>21,25</sup> The relative ease with which DOCT can image dilated blood vessels in HHT suggests, therefore, that DOCT might be useful in angiogenesis research.

The patients in the present study, with hemorrhage-prone MCT, described typical telangiectatic bleeding.<sup>21</sup> Hemorrhage usually occurred without any apparent trauma or with only minor local irritation, and the bleeding was arteriolar, that is, profuse and

spurting. Among the MCT imaged, there was a relationship between shallow MCT depth and increased tendency to bleed. Two of 3 cutaneous telangiectases with a bleeding history had penetrated the stratum spinosum layer on DOCT imaging, possibly indicating that the keratin layer prevents MCTs from bleeding. Lesions with a bleeding history ranged from small to large in size, possibly implying that, as MCTs enlarge, the surface-to-lesion distance decreases, leading to the thinning of the overlying tissue, so that the probability of hemorrhage with local trauma increases. It is unknown whether larger MCTs are more fragile than smaller MCTs. If this is true, larger MCTs will tend to bleed into the dermis and mucosa more easily than small lesions regardless of depth. However, in clinical practice, it is uncommon to observe intracutaneous or intramucosal hemorrhage surrounding large MCTs. Hence, the depth of the MCTs plays a pivotal role in the tendency to bleed.

Nine telangiectases in the nail folds of 9 patients with HHT were imaged, and DOCT unequivocally detected the vascular lesions, while no abnormal Doppler signal was found in normal surrounding nail folds. Mager and Westermann<sup>27</sup> used light microscopy (16× to 40×) to study the giant capillary loops seen in the nail folds of patients with HHT and other connective tissue diseases. Eighty-three percent of the patients with HHT had giant capillary loops between the normal capillaries, whereas no normal volunteer had such loops. The loops were either not visible or barely visible. In the current study, the vascular loops were not visible by eye or DOCT. No abnormal Doppler signals were found in the normal areas surrounding these MCTs and 5 additional sites. Perhaps the flow velocity and blood volume in these loops are similar to those within normal capillaries, so that DOCT was unable to detect them. It is unknown whether these vascular loops represent early skin changes preceding detectable MCTs.

The proportion of patients with pulmonary AVMs (8/12, 66.7%) was relatively high in the present study. Referral bias is likely responsible because all patients were recruited from a HHT clinic where they were followed on a regular basis. Among systematically screened HHT populations, pulmonary AVMs are found in approximately 30% of patients.<sup>28</sup>

In summary, the abnormal vascular structure and flow dynamics of MCTs in HHT were easily detected and visualized with DOCT, which unequivocally demonstrated MCTs as globular shapes with high volume and/or blood flow velocity. In contrast, normal superficial blood vessels were rarely detectable with DOCT, and the few normal vessels

that were visualized were extremely small. No abnormal structure or Doppler signal was found in visually normal areas of the skin of patients with HHT. Mucocutaneous telangiectases with a bleeding history were situated closer to the stratum spinosum than lesions that had not bled. DOCT is a noninvasive procedure. Less than one minute is required to examine each site. DOCT is potentially useful for the diagnosis of mucocutaneous vascular lesions and neovascularity, and potentially could guide therapeutic interventions. Based on these results, DOCT will be applied endoluminally to investigate HHT in the GI tract, neovascularity associated with mucosal dysplasia and cancer, GAVE, portal hypertensive gastroenteropathy, and other mucosal and submucosal vascular disorders.

#### ACKNOWLEDGMENTS

This work was supported by Natural Science and Engineering Research Council of Canada, Canadian Institutes for Health Research, Canada Foundation of Innovation and Photonics Research Ontario. Financial support for Dr. Marie E. Faughnan includes the Squires Club, St. Michael's Hospital Research Institution, and the Sonor Foundation.

#### REFERENCES

1. Guttmacher AE, Marchuk DA, White RI Jr. Hereditary hemorrhagic telangiectasia [review]. *N Engl J Med* 1995;333:918-24.
2. Shovlin CL, Guttmacher AE, Buscarini E, Faughnan ME, Hyland RH, Westermann CJ, et al. Diagnostic criteria for hereditary hemorrhagic telangiectasia (Rendu-Osler-Weber syndrome). *Am J Med Genet* 2000;91:66-7.
3. Plauchu H, de Chadarevian JP, Bideau A, Robert JM. Age-related clinical profile of hereditary hemorrhagic telangiectasia in an epidemiologically recruited population. *Am J Med Genet* 1989;32:291-7.
4. Kjeldsen AD, Kjeldsen J. Gastrointestinal bleeding in patients with hereditary hemorrhagic telangiectasia. *Am J Gastroenterol* 2000;95:415-8.
5. Bergler W, Sadick H, Gotte K, Riedel F, Hormann K. Topical estrogens combined with argon plasma coagulation in the management of epistaxis in hereditary hemorrhagic telangiectasia. *Ann Otol Rhinol Laryngol* 2002;111:222-8.
6. Dave RU, Mahaffey PJ, Monk BE. Cutaneous lesions in hereditary haemorrhagic telangiectasia: successful treatment with the tunable dye laser. *J Cutan Laser Ther* 2000;2:191-3.
7. Tearney GJ, Brezinski ME, Bouma BE, Boppart SA, Pitris C, Southern JF, et al. In vivo endoscopic optical biopsy with optical coherence tomography. *Science* 1997;276:2037-9.
8. Tearney GJ, Brezinski ME, Southern JF, Bouma BE, Boppart SA, Fujimoto JG. Optical biopsy in human gastrointestinal tissue using optical coherence tomography. *Am J Gastroenterol* 1997;92:1800-4.
9. Chen Z, Milner TE, Wang X, Srinivas S, Nelson JS. Optical Doppler tomography: imaging in vivo blood flow dynamics following pharmacological intervention and photodynamic therapy. *Photochem Photobiol* 1998;67:56-60.
10. Sivak MV Jr, Kobayashi K, Izatt JA, Rollins AM, Ung-runyawee R, Chak A, et al. High-resolution endoscopic imaging of

- the gastrointestinal tract using optical coherence tomography. *Gastrointest Endosc* 2000;51:474-9.
11. Poneros JM, Brand S, Bouma BE, Tearney GJ, Compton CC, Nishioka NS. Diagnosis of specialized intestinal metaplasia by optical coherence tomography. *Gastroenterology* 2001;120:7-12.
  12. Nelson JS, Kelly KM, Zhao Y, Chen Z. Imaging blood flow in human port-wine stain in situ and in real time using optical Doppler tomography. *Arch Dermatol* 2001;137:741-4.
  13. Wong RC, Yazdanfar S, Izatt JA, Kulkarni MD, Barton JK, Welch AJ, et al. Visualization of subsurface blood vessels by color Doppler optical coherence tomography in rats: before and after hemostatic therapy. *Gastrointest Endosc* 2002;55:88-95.
  14. Yang VXD, Gordon ML, Qi B, Seng Yue E, Tang SJ, Bisland SK, et al. High sensitivity detection and monitoring of micro-circulation using cutaneous and catheter probes for Doppler optical coherence tomography. *Proc SPIE* 2003;4965:153-9.
  15. Yang VXD, Pekar J, Lo SW, Gordon ML, Mok A, Wilson BC, Vitkin IA. Optical coherence and Doppler tomography for monitoring tissue changes induced by laser thermal therapy an in vivo feasibility study. *Rev Sci Instrum* 2003;74:437-40.
  16. Yang VXD, Gordon ML, Mok A, Zhao Y, Chen Z, Cobbold RSC, et al. Improved phase-resolved optical Doppler tomography using the Kasai velocity estimator and histogram segmentation. *Opt Commun* 2002;208:209-14.
  17. Kobayashi K, Izatt JA, Kulkarni MD, Willis J, Sivak MV Jr. High-resolution cross-sectional imaging of the gastrointestinal tract using optical coherence tomography: preliminary results. *Gastrointest Endosc* 1998;47:515-23.
  18. Seitz U, Freund J, Jaeckle S, Feldchtein F, Bohnacker S, Thonke F, et al. First in vivo optical coherence tomography in the human bile duct. *Endoscopy* 2001;33:1018-21.
  19. Poneros JM, Tearney GJ, Shiskov M, Kelsey PB, Lauwers GY, Nishioka NS, Bouma BE. Optical coherence tomography of the biliary tree during ERCP. *Gastrointest Endosc* 2002;55:84-8.
  20. Shim MG, Wong LM, Marcon NE, Wilson BC. In vivo near-infrared Raman spectroscopy: demonstration of feasibility during clinical gastrointestinal endoscopy. *Photochem Photobiol* 2000;72:146-50.
  21. Braverman IM, Keh A, Jacobson BS. Ultrastructure and three-dimensional organization of the telangiectases of hereditary hemorrhagic telangiectasia. *J Invest Dermatol* 1990;95:422-27.
  22. Jahnke V. Ultrastructure of hereditary telangiectasia. *Arch Otolaryngol* 1970;91:262-5.
  23. Menefee MG, Flessa HC, Glueck HI, Hogg SP. Hereditary hemorrhagic telangiectasia (Osler-Weber-Rendu disease). An electron microscopic study of the vascular lesions before and after therapy with hormones. *Arch Otolaryngol* 1975;101:246-51.
  24. Sawabe M, Arai T, Esaki Y, Tsuru M, Fukazawa T, Takubo K. Three-dimensional organization of the hepatic microvasculature in hereditary hemorrhagic telangiectasia. *Arch Pathol Lab Med* 2001;125:1219-23.
  25. Jacobson BS. Hereditary hemorrhagic telangiectasia: a model for blood vessel growth and enlargement [review]. *Am J Pathol* 2000;156:737-42.
  26. Folkman J. Tumor angiogenesis and tissue factor [letter]. *Nat Med* 1996;2:167-8.
  27. Mager JJ, Westermann CJ. Value of capillary microscopy in the diagnosis of hereditary hemorrhagic telangiectasia. *Arch Dermatol* 2000;136:732-4.
  28. Nanthakumar K, Graham AT, Robinson TI, Grande P, Pugash RA, Clarke JA, et al. Contrast echocardiography for detection of pulmonary arteriovenous malformations. *Am Heart J* 2001;141:243-6.